Chapter 16

A Heart to Heart Discussion: Cardiac MRI

16.1 Introduction

Cardiac MRI has always been one of the most challenging clinical applications. Imaging in the presence of cardiac and respiratory motion as well as blood flow has required the development of robust methods to obtain good-quality images in patients who, by definition, have have irregular ECGs, and often present with difficulties in holding their breath. Fortunately continued developments in system hardware, pulse sequences and reconstruction algorithms have improved the reliability of standard imaging methods and have also introduced new techniques for myocardial tissue characterization. Given these technical advancements, challenges remain for the user in understanding and optimizing the sequences and methods.

In this chapter we will explain that:

- good patient preparation is important for obtaining high-quality cardiac studies;
- 'dark-blood' imaging techniques provide morphological scans of the heart;
- 'bright-blood' cine imaging methods are used to assess global and regional ventricular cardiac function;
- contrast-enhanced MRI can be used to evaluate myocardial ischaemia and viability.

16.2 Patient Set-up

Historically, cardiac MRI has often been considered as 'difficult'. However, modern scanners have removed much of the mystique and complexity of performing cardiac imaging. The major technical challenges arise from motion: of the heart itself, pulsatile blood flow and respiratory motion. Many artefacts arise because of changes in signal intensity or phase with time and commonly result in ghosting artefacts.

The most effective method to reduce motion is to trigger or gate the acquisition to the patient's physiology. Triggering is usually used to describe a sequence that is started by a particular event, such as the scanner hardware detecting an ECG 'trigger', while gating is used to describe a method where data are only acquired during a particular time period, or 'gate', such as during a quiet period of the patient's breathing. However, the terms gating and triggering are often used interchangeably.

ECG triggering is used so that data are always acquired in the same part of the cardiac cycle so ideally the position of the heart is the same. This requires a good-quality ECG waveform for the MRI system to detect the R-wave and trigger the acquisition (see Box 'Perfect Gating Needs Good Preparation'). Obtaining a good ECG inside the bore of an MRI system is not easy, for two reasons: first, the electrodes need to be placed reasonably close together to avoid large differential voltages being induced in the cables by the gradients and RF; and second, the ECG waveform itself is distorted through the magneto-hydrodynamic effect: an additional voltage induced by blood (a conducting fluid) moving within a magnetic field. Since the fastest blood flow in the aorta occurs at the time of ventricular ejection, this additional voltage is superimposed on the T-wave of the ECG. The amplitude of the T-wave may then be greater than that of the R-wave, resulting in incorrect triggering.

Fortunately, ECG triggering has become significantly more reliable through the widespread use of **V**ector **C**ardiac **G**ating (VCG), as shown in Figure 16.1. Four electrodes are placed in a cross arrangement so that there is a left–right signal component (x) and a superior–inferior signal component (y). Simultaneously acquiring both components allows the direction of the R-wave to be tracked as it moves with the cardiac cycle. It has been shown that

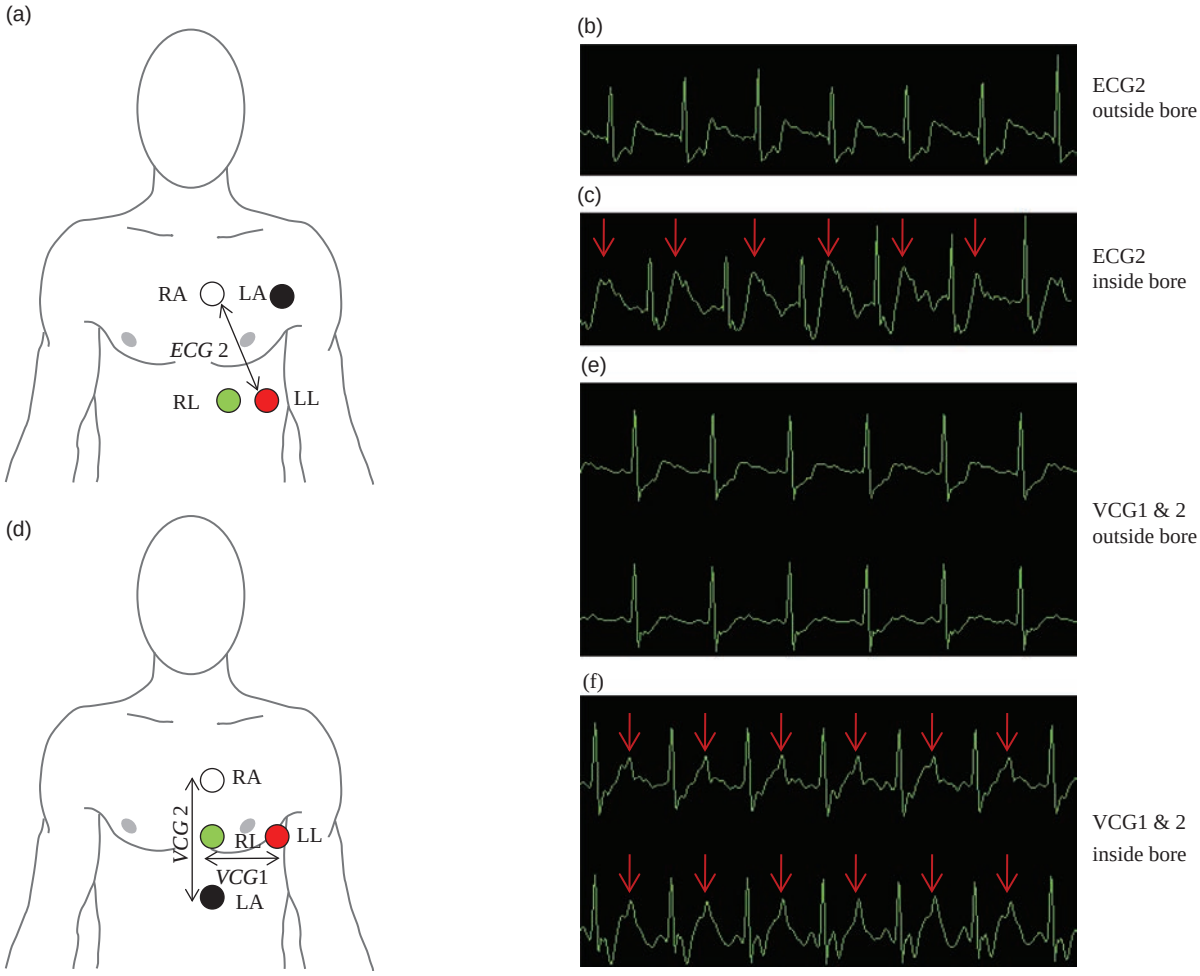

Figure 16.1 ECG gating. (a) Original ECG electrode placement to obtain a standard Lead II ECG (ECG2). (b) This arrangement can produce an acceptable waveform outside of the magnet. (c) Inside the bore of the magnet the magneto-hydrodynamic effect means that the T-wave can increase in amplitude (arrows). This may cause false triggering. (d) Electrode arrangements for vector electrocardiogram (VCG). The electrodes are positioned in a crossed arrangement so that there is a left–right signal component (x – VCG1) and a superior–inferior signal component (y – VCG2). (e) Outside of the magnet the waveforms are good. (f) Inside the bore of the magnet there is still a larger T-wave (arrows), but signal processing of both the VCG1 and VCG2 waveforms can reduce false triggering.

the electrical vector of the heart tracks a different path to that of the magneto-hydrodynamic artefact. Appropriate signal processing of both the spatial and temporal changes of these 2D vectors significantly improves the triggering reliability compared to just using a standard ECG.

To overcome respiratory motion, nowadays we usually make sure that the entire data collection is acquired in a single breath-hold. However sequences that cannot be made fast enough, e.g. some 3D acquisitions, may require respiratory triggering. This is typically achieved by the use of either a pneumatic bellows positioned around the patient's chest, or by respiratory navigators. The respiratory signal from the bellows triggers the MRI acquisition when the patient's chest movement is relatively quiet, i.e. at end expiration. You typically select the desired trigger point of the acquisition as well as the repeat time in terms of the number of respiratory cycles. While the bellows are an indirect method of monitoring respiration, a navigator is an MR method for directly tracking the motion of the diaphragm.

A navigator is a mini pulse sequence that excites and receives the MR signal from a one-dimensional

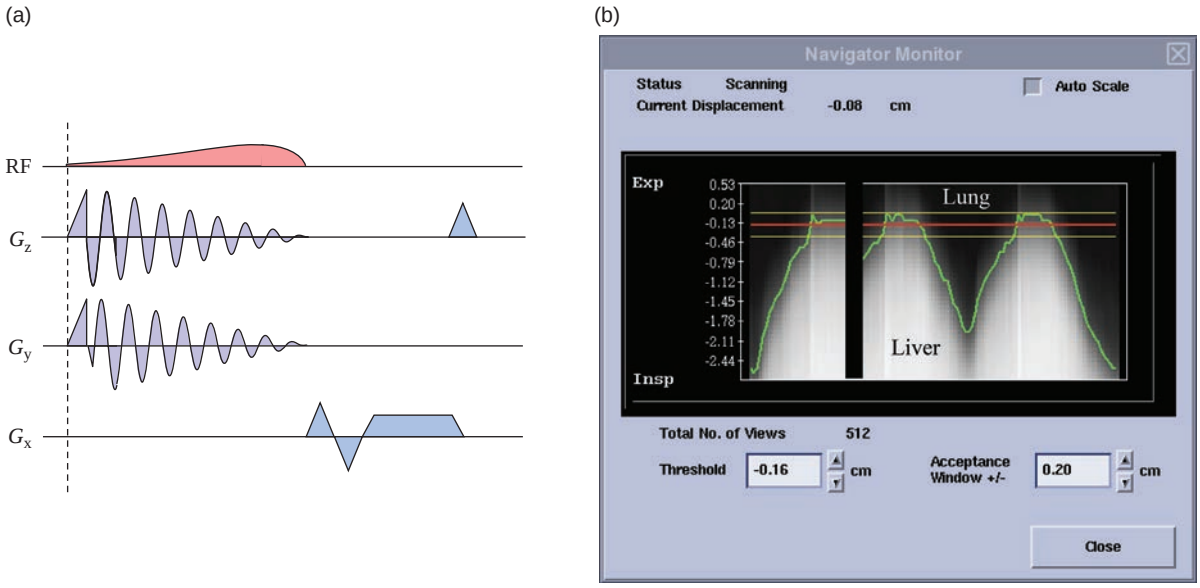

Figure 16.2 Navigator echoes. (a) 2D cylindrical navigator pulse sequence. The navigator is positioned on the dome of the left hemidiaphragm. (b) Typical navigator output. The bright signal below the green line is the liver, while the darker signal above is the lung. The two yellow parallel lines represent the acceptance window and the red line the threshold.

column of spins usually positioned on the right hemidiaphragm (see Box 'Navigating the Pulse Sequence'). The signal is Fourier transformed and shows the contrast between the lung (dark) and the diaphragm/upper edge of the liver (bright). The navigator initially monitors the patient's diaphragm motion and establishes a user-controllable acceptance window. Once the imaging sequence is started, the navigators are played out repeatedly until the diaphragm position falls into the acceptance window, at which point a proportion of the total data acquisition is performed. In more sophisticated applications the diaphragm position is monitored before and after the image acquisition, and data are rejected if the post-acquisition navigator indicates that the diaphragm has moved out of the acceptance window during the image acquisition. Figure 16.2 shows the sequence and data acquisition for a navigator.

The use of multiple channel coil arrays that can exploit parallel imaging techniques has made a particularly big impact on cardiac imaging. Parallel imaging can be used, for example, to reduce the overall acquisition time, or to improve the temporal resolution or coverage of a particular acquisition. All the methods described in this chapter can be accelerated and you should work with your system vendor to optimize their use on your particular system.

Perfect Gating Needs Good Preparation

The key to obtaining a good triggering waveform is to spend some time preparing the electrode sites. First, any chest hair should be removed with a razor; second, the skin should be gently abraded using an appropriate gel to strip away the top layer of skin and moisten the underlying layer. This reduces the skin impedance and improves the electrical conductivity. Appropriate MRI-safe ECG electrodes and leads should always be used. Poor VCG signal is the single largest cause of failed cardiac MR exams. Your manufacturer will often have special advice, and you should take some time to practice electrode positioning to make sure you do everything you can to get it right every time.

If it is not possible to obtain an adequate ECG trigger, then **P**eripheral **G**ating (PG) could be used for triggering, using a photoplethysmograph, often just called the 'pleth', positioned on a finger or toe. However, it should be noted that there is a significant delay (150–500 ms) between the R-wave of the ECG and the peak of the peripheral pulse. The PG signal simply reflects the change in blood volume through the vessels in the finger or toe and is therefore insensitive to magnetic field effects. Note that images acquired immediately after the PG trigger will fall in diastole and that systole may be lost in any arrhythmia rejection (AR) period at the end of the PG cycle.

Navigating the Pulse Sequence

Navigators involve some unusual methods for pulse sequence programming. The first question is how do you excite a column? The first possibility is a spin-echo sequence with orthogonal slice-selective gradients on the 90° and the 180° pulses, thus the spin-echo signal only arises from the column of spins where the two intersect. The column can be freely positioned and angled, but has the disadvantage of creating black bands where the navigator selection intersects with the main image – possibly right through the anatomy of interest.

The alternative is a 2D excitation, as shown in Figure 16.2. The alternating gradients during the RF pulse excite a circular column, often known as a pencil beam. Since it's a gradient echo, it can be used with a shorter TR and less SAR than the spin-echo technique.

16.3 Morphological Imaging

Most morphological imaging is done with ECG-triggered fast/turbo spin echo acquired in a breath-hold. Since the duration of a TSE echo train may be relatively long, data acquisition is usually performed in diastole when cardiac motion is minimized. Unfortunately blood within the cardiac chambers is also stationary in diastole, and this can result in undesirable high signal from stationary blood within the ventricles. To overcome this, we use a **D**ouble **I**nversion **R**ecovery (DIR) scheme before the TSE acquisition, known as blood suppression, dark blood or black blood preparation. Figure 16.3 shows the principles of DIR blood suppression. The DIR preparation starts with a non-selective 180° pulse, which inverts spins in the entire imaging volume. This is immediately followed by a

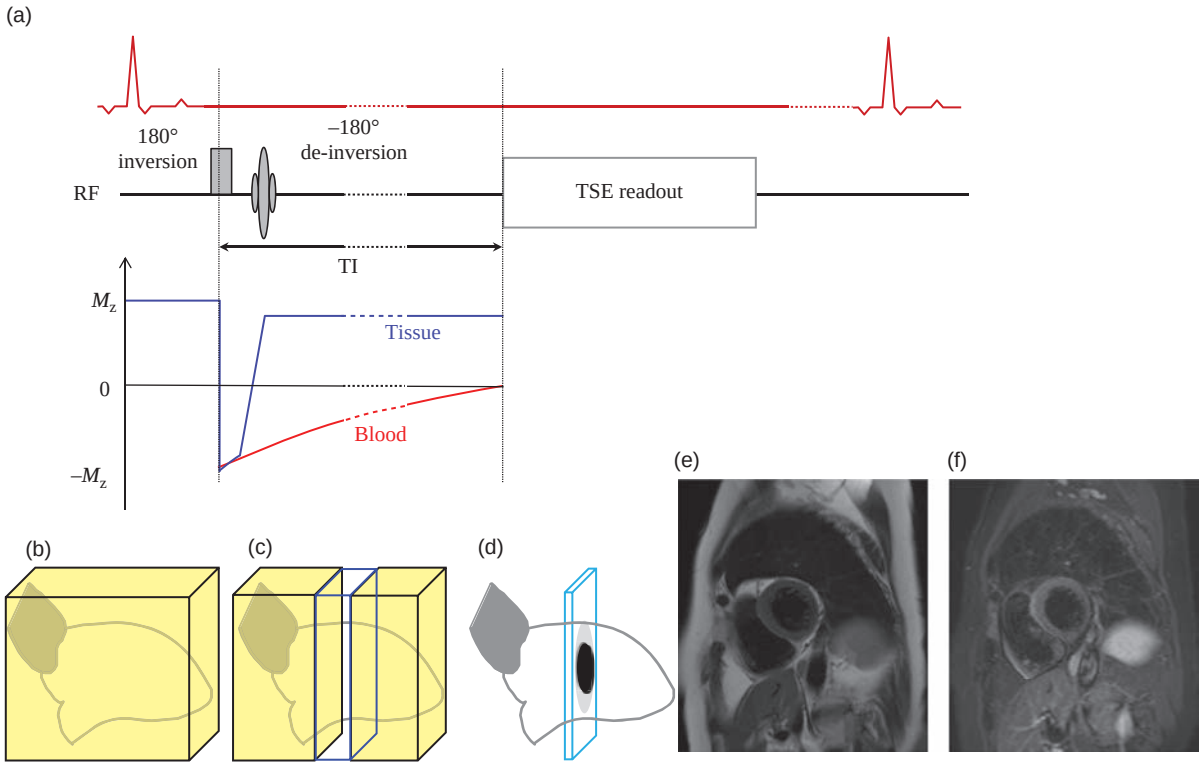

Figure 16.3 Principles of black-/dark-blood suppression. In (a) the first non-selective 180° inversion pulse inverts all the magnetization (b). This is immediately followed by a slice-selective 180° de-inversion that returns the tissue signal back to equilibrium (c). However, the blood outside the de-inversion slice remains inverted. During the TI time blood washes out of the de-inverted slice and inverted blood washes in. The TI is chosen so that the readout is applied when the M_z magnetization of blood crosses zero. The readout slice thickness (d) is thinner than the de-inversion slice thickness to account for myocardial motion during the TI time. The resultant image (e) demonstrates good blood suppression. A third inversion pulse can also be included, which can be used to suppress the signal from fat (f), to give a fat- and blood-suppressed image.

slice-selective 180° de-inversion. The goal is to invert all the spins outside of the imaging slice, while the static spins within the slice experience both the inversion and the de-inversion, i.e. they are effectively unchanged. There is a delay time TI before the start of the TSE sequence, which fulfils two requirements: first, blood within the imaging slice will wash out of the slice and be replaced by inverted blood; second, the inverted blood will recover due to T_1 relaxation. As you might expect, the TI is calculated so that at the image acquisition the blood is at the null point, giving no signal. If all the blood in the slice is replaced by in-flowing blood during TI, we will get a perfect 'black blood' appearance within the ventricles. Note that blood that is not replaced during the TI period, i.e. very slow-flowing blood, or blood flow that is mainly in-plane, may not be completely suppressed. The TI is normally calculated based on literature values for T_1 of blood (around 1400 ms at 1.5 T, and 1600 ms at 3 T), but it also depends on the duration of the echo train, and the TR (generally one or two R-to-R-wave intervals). Therefore black-blood preparation schemes are not easy to use post-Gd, since the T_1 of blood will be reduced to an unknown value.

DIR preparation can also be combined with single-shot turbo spin echo (SS-TSE) or HASTE. This allows a complete image to be acquired in a single heartbeat, and therefore multiple images can be acquired in a single breath-hold. These scans are typically used for cardiac localizers or scouts.

A third slice-selective 180° pulse can also be incorporated into the sequence preparation to give a STIR contrast mechanism. This permits fat-suppressed images to be obtained with the benefits of a blood-suppressed, breath-hold TSE acquisition. T_2-STIR is widely used to assess the oedema associated with acute myocardial infarction, with the size of the T_2 abnormality correlating with the so-called area-at-risk (AAR), the region of the myocardium that may or may not go on to infarction.

16.4 Functional Imaging

Functional cardiac imaging is designed to visualize the heart motion throughout the cardiac cycle. We use gradient-echo sequences for this, triggered by the VCG. Gradient-echo sequences have very short repetition times (TR), so data from the same slice location can be acquired at different time-points through the cardiac cycle. Each time-point is known as a 'cardiac phase' or 'temporal phase'. Thanks to the flexibility of MR slice selection, it is possible to acquire multiphase 'cine' images in any plane. For example, a properly positioned four-chamber view demonstrates the function of the left and right ventricles and atria as well as the tricuspid and mitral valves in the same slice. From this plane a stack of **S**hort **A**xis (SA) cine images encompassing the entire left ventricle can be obtained. The SA view is the preferred orientation for the study of global and regional ventricular function. Another commonly used orientation is the **L**eft **V**entricular **O**utflow **T**ract (LVOT) view which allows visualization of blood entering and leaving the left ventricle. There are some special MR techniques unique for cardiac cine imaging, explained in the following sections.

Finding Your Way with Cardiac Planes

Cardiac MRI does not typically use standard, axial, sagittal and coronal views. Most imaging planes are double oblique, orientated to the heart chambers and the valves. Obtaining these standard views requires a good knowledge of cardiac anatomy and lots of practice. Figure 16.4 shows the slice prescriptions in order to obtain the main cardiac planes. Each image is a single (end-diastolic) phase from a 20 temporal-phase cine acquisition.

16.4.1 Balanced Steady-State-Free-Precession

In the early days of cardiac MRI, cine imaging used spoiled gradient-echo sequences. These sequences relied on the in-flow of blood to provide the contrast between the bright blood-pool and the darker myocardium; hence image quality could be quite variable. Cardiac MRI was therefore substantially improved with the development of cine balanced steady-state-free-precession (bSSFP), a fully rewound GE sequence. As in the MRA world, 'bSSFP' is widely used as the generic term in the cardiac MR world, so in this chapter we will follow the same convention. Since the contrast in bSSFP depends mainly on the ratio T_2/T_1, the contrast between blood (where the ratio is high) and myocardium (where it is less), is much better. You might know bSSFP as FIESTA, bFFE or True-FISP, depending upon your scanner.

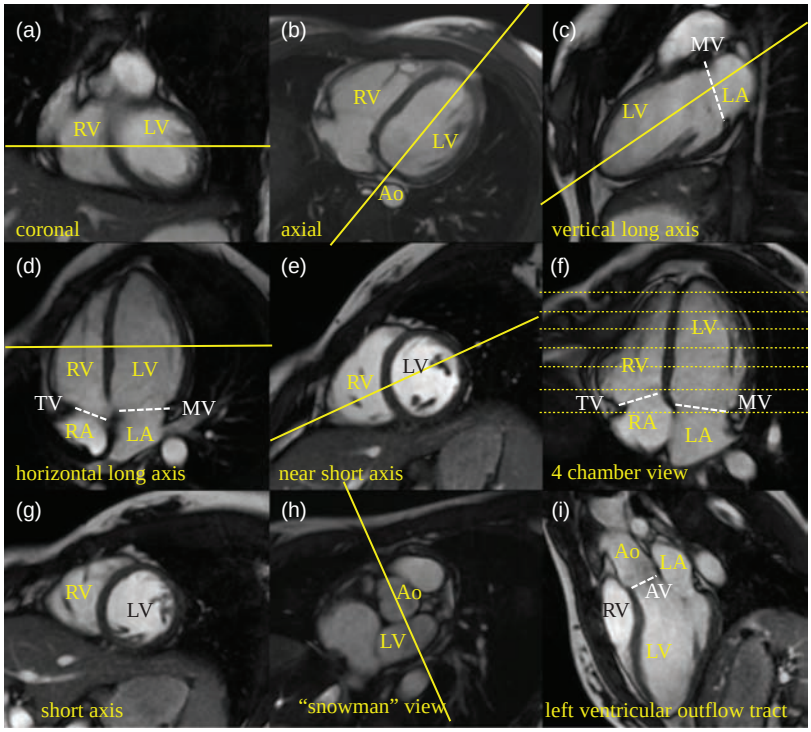

Figure 16.4 Cardiac planes prescription, starting from (**a**) a coronal view. From this an axial slice through the left ventricle (LV), right ventricle (RV) and aorta (Ao) is obtained (b). (**b**) An oblique slice through the centre of the LV parallel to the septum, to create a vertical long axis (VLA) view (c). (**c**) An oblique slice through the apex of the LV and the middle of the mitral valve (MV), which creates a horizontal long axis (HLA) view showing the right atrium (RA), left atrium (LA), MV and the tricuspid valve (TV) (d). (**d**) A slice perpendicular to the septum obtains a near short axis slice (e). An oblique slice through the centre of the LV and the inferior margin of the RV obtains the standard four-chamber view (4CH). The standard stack of short axis slices (dotted lines) is then prescribed on this 4CH view, perpendicular to the septum. A typical mid-ventricular short axis slice is shown in (**g**). (**h**) A more basal short axis slice demonstrating the 'snowman' view of the Ao and top of the LV. (**i**) An oblique slice through the middle of the snowman results in the view of the left ventricular outflow tract (LVOT) which shows the aortic valve (AV).

16.4.2 Segmented k-Space Acquisitions

Ideally we would like to acquire all the data for each multiphase cine slice in a single breath-hold. Each temporal phase involves the acquisition of a number of phase-encoding steps, similar to the echo-train length in turbo spin echo. Unfortunately different manufacturers use different terms to refer to this method, which has enormous potential to confuse both us (the authors) and you (the reader). We will therefore make our own definitions, as follows: an individual phase encoding is called a 'view' and the number of views that make up an individual temporal phase as the 'echo train length' (ETL). This technique of acquiring multiple views in a single R–R interval is called segmented k-space imaging. The basic principles of segmented k-space cine imaging are shown in Figure 16.5.

Let's use an example to show how segmented k-space imaging works. We will acquire a multiphase cine acquisition with a frequency × phase matrix of 256 × 128, i.e. each cine phase comprises 128 views. If we acquire one view per temporal phase in each heartbeat then the total acquisition time would be 128 heartbeats. If the heart rate was 60 bpm, i.e. the *R–R* interval was 1000 ms in duration, then the acquisition time would be over 2 min, which is certainly not a breath-hold. However, since the individual TR for each bSSFP view might only be 3.5 ms, we could theoretically acquire 1000/3.5 ≈ 285 temporal phases. That's far more than we really need, so it would make sense to acquire more than one view per temporal phase in each *R–R* interval. Suppose that instead of collecting one view per temporal phase we collect 12, i.e. we make the ETL = 12. The overall acquisition time is now only 128/12 ≈ 11 heartbeats, which is a reasonable breath-hold time of 11 s. The data acquisition time for each ETL, i.e. the effective temporal resolution, would now be 3.5 × 12 = 42 ms, and the maximum number of temporal phases we could acquire would be 1000 ÷ 20 ≈ 23.

In keeping with our TSE analogy, some manufacturers, such as Siemens, refer to the 42 ms duration of each temporal phase as the 'TR' and the duration of each view (3.5 ms) as the echo-spacing (ESP), i.e. the TR = ETL × ESP. The choice of ETL in practice will depend upon how long the patient can hold their breath and the amount of acceptable artefact, i.e. blurring and ghosting due to motion, which can occur during each temporal phase.

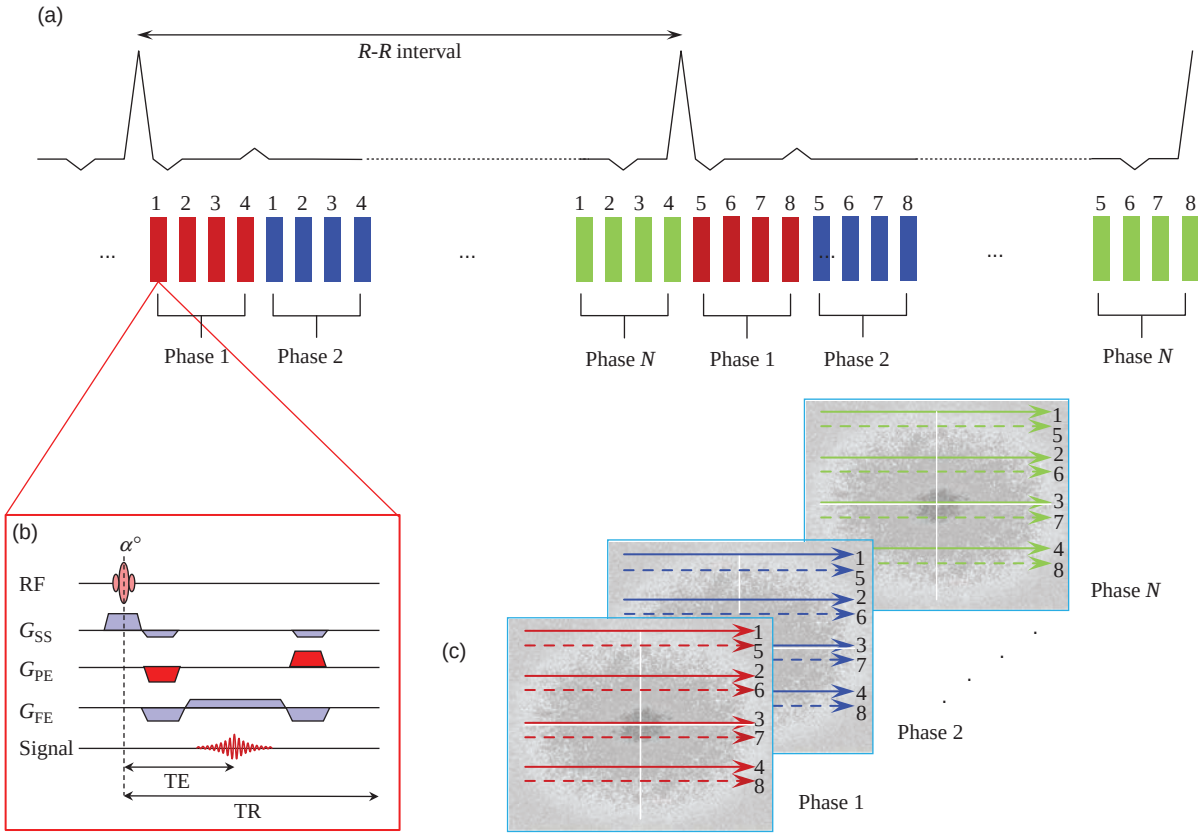

Figure 16.5 Segmented k-space cardiac imaging. In order to reduce the overall acquisition time a number of phase-encoding steps, or views, are acquired in the same heartbeat. Each line in (a) represents a single TR balanced steady-state-free-precession gradient-echo sequence (b) with a specific phase-encoding gradient amplitude. In this case four views are acquired for each raw data temporal phase (c) per *R–R* interval.

16.4.3 Prospective and Retrospective Cine Imaging

So far we have assumed that the heart rate does not change for the 11 heartbeats that are required to fully complete the cine scan. In reality many patients have arrhythmias which means that their heart rate may vary during the scan. Any heartbeat that is shorter than normal will result in incomplete data acquisition. A simple way to prevent this is to monitor the patient's heart rate for a few beats to establish its variability. The user can then set a period known as the **A**rrhythmia **R**ejection **P**eriod (ARP) shown in Figure 16.6, during which the data acquisition will be disabled. The ARP is typically 10–20% of the duration of the average *R–R* interval. This allows the *R–R* interval to vary within the ARP without the data from the arrhythmic heartbeat being rejected. In order to maintain the magnetization in a steady state the pulse sequence continues to play out during the ARP; it is just data acquisition that is disabled. This method is known as prospective triggering since the system looks for the next R-wave trigger after the ARP to occur. Any data that are acquired when an *R–R* interval falls outside of the arrhythmia rejection window are discarded and reacquired. The disadvantage of prospective gating is that data are not acquired during the ARP and therefore we may miss important information about ventricular function during end-diastole.

The alternative to prospective triggering is retrospective gating, in which data are acquired throughout the cardiac cycle, including the ARP, and the duration of each heartbeat is recorded. The arrhythmia rejection window may be much larger, typically 50%, so fewer beats are discarded. Any variation in *R–R* interval length is addressed by the retrospective processing. After the scan is complete, each heartbeat

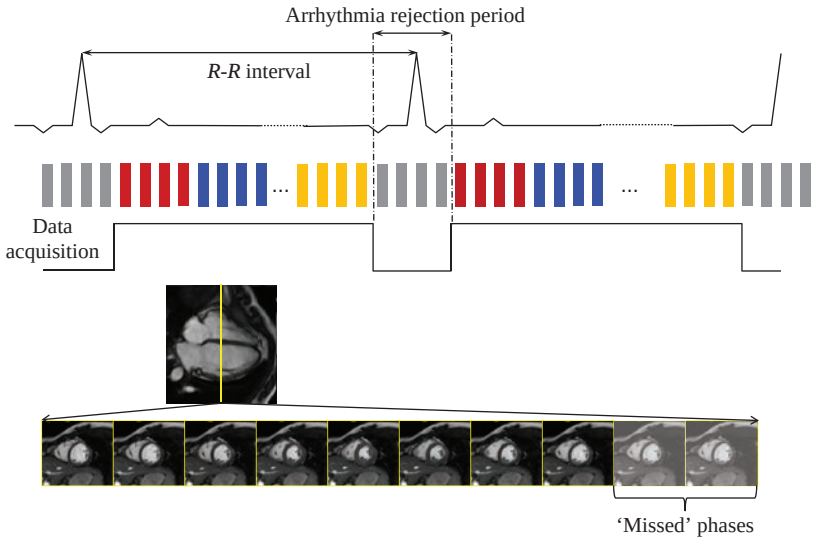

Figure 16.6 Prospective gating. Data acquisition is initiated or triggered by the ECG; however, data acquisition is turned off during the arrhythmia rejection period, typically 10–20% of the nominal *R–R* interval. Phases at the end of the cardiac cycle are therefore missed. The pulse sequence continues to play out during the arrhythmia rejection period (grey segments) to ensure that the magnetization remains in the steady state. Any data that are acquired when an *R–R* interval falls outside of the arrhythmia rejection window are discarded and reacquired.

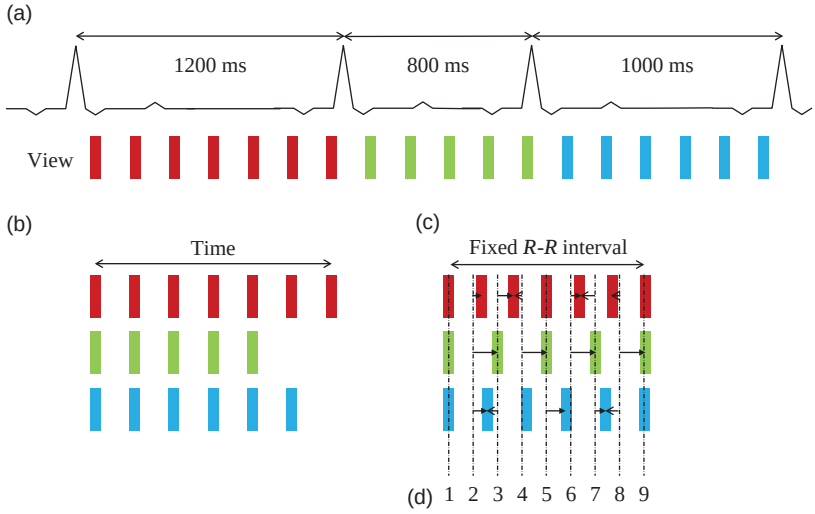

Figure 16.7 Retrospective processing. (**a**) Three consecutive heartbeats have different *R–R* intervals. Each line represents one phase encoding step or view, i.e. this example shows three different views (red, green and blue), each acquired in a different heartbeat. (**b**) This results in a different number of views for each heartbeat. (**c**) In retrospective processing, each *R–R* interval is made the same fixed length by either contracting or stretching the cardiac cycle. The user decides on an arbitrary number of reconstructed phases, in this case nine. (**d**) The nearest temporally acquired view for each of the reconstructed phases is then selected. Arrows are used to show the nearest-neighbour view where necessary. Note that some views are used for two adjacent reconstructed phases to ensure that each phase has three views.

is stretched or compressed to match the nominal *R–R* interval, and the time-point of each view (or ETL) is re-assigned as shown in Figure 16.7. The data are retrospectively allocated to a new, user-defined, number of temporal phases, independent of the number of actually acquired phases. A simple approach for allocating acquired temporal views to the new user-defined temporal phase is to use the nearest-neighbour algorithm. Since the relative time of acquisition of each acquired view may no longer be the same, it may be necessary for the same acquired temporal view to be used in adjacent user-defined phases, but the reconstruction ensures that the whole cardiac cycle is fully sampled. Retrospective gating still uses an ARP, but it is typically much bigger, e.g. 50% of the average *R–R* interval, than the value used for prospective triggering. Therefore only very short or very long beats will be rejected.

16.4.4 View Sharing

Sometimes it is necessary to increase the ETL in order to keep the scan acquisition time short. When this happens the effective temporal resolution will be decreased, resulting in blurring in the images or jerkiness in cine movies. To maintain a good temporal

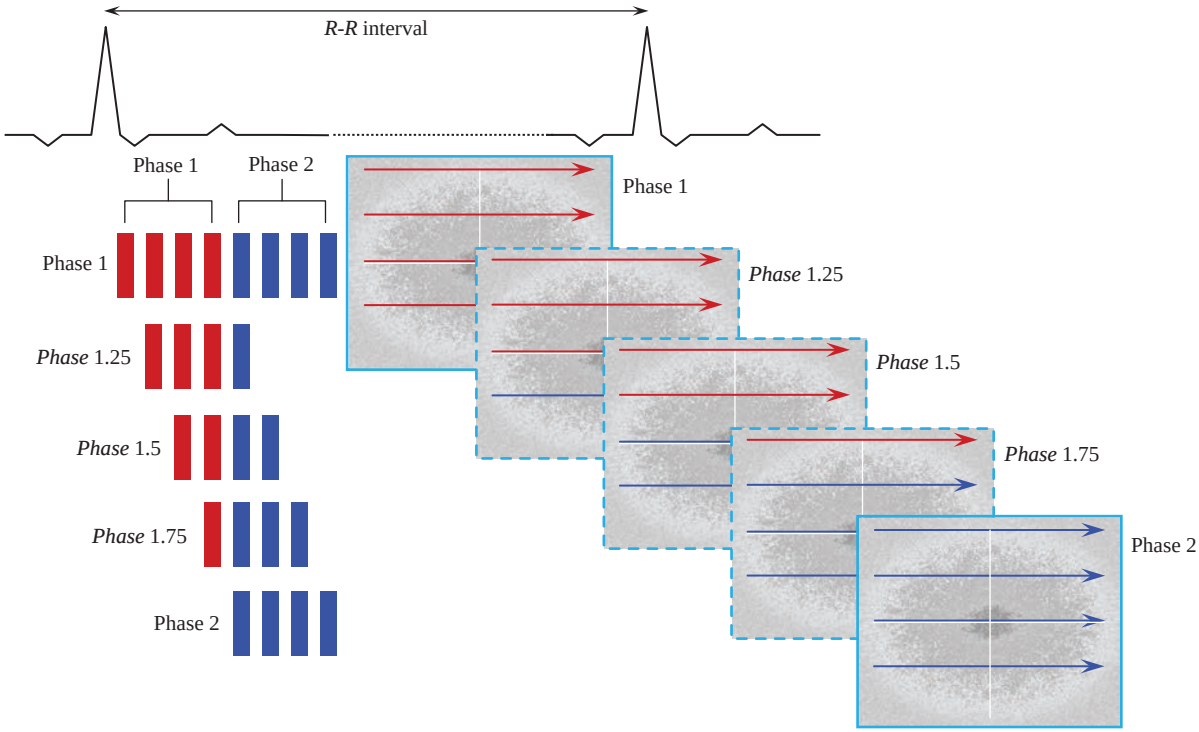

Figure 16.8 Variable view sharing. In this example there are four phase-encoding steps, or views, acquired for each temporal phase in the same *R–R* interval. The diagram shows that phase 1 is made up of the four red views and phase 2 is made up of the four blue views. Additional intermediate temporal phases can be synthesized by 'sharing' the views between phases 1 and 2. The diagram shows how varying numbers of views from phase 2 can be shared with phase 1 to create additional phases. Note that there is no additional data acquisition, only that the original data are shared.

resolution we can use a technique known as 'view sharing' (also known as 'echo sharing'). With view sharing, the lines of raw data from adjacent temporal phases are combined to synthesize an intermediate temporal phase image. For example, if we now consider an ETL of 8, we can combine the last four views of phase n with the first four views of phase $n + 1$ to produce a new temporal phase with eight views. The time-point of this new phase will be positioned at $1/2(t_n + t_{n+1})$. Using this equal (or symmetric) view sharing, the total number of temporal phases can be increased from N to $2N - 1$. There is of course no reason why views could not be asymmetrically, or variably, shared; for example, the last two views from phase n with the first six views of phase $n + 1$ to generate a new temporal phase positioned at $3/4(t_n + t_{n+1})$. However, you should be aware that view sharing does not create new data, it is performing temporal interpolation between the real acquired phases to generate intermediate steps. View sharing definitely helps to produce smoother cine movies. Figure 16.8 illustrates how variable view sharing can be used to create additional interpolated temporal phases. Variable view sharing is particularly useful in retrospectively gated acquisitions where there is a need to share the views appropriately to match the number of desired user-defined temporal phases.

Real-Time Cine Imaging

It is important to realize that although cine images show function over a single cardiac cycle, the raw data are actually acquired over a number of heartbeats, meaning that a reasonably stable heart rate is needed in order to obtain good-quality images. If this is not the case, e.g. with patients in atrial fibrillation, then it is possible to acquire images rapidly enough to demonstrate cardiac function without using ECG triggering or gating. These methods are often referred to as real-time cine imaging. If an entire image can be acquired rapidly enough then it is possible to acquire sequential images at around 8–12 frames per second. In order to acquire at a sufficiently good temporal resolution it is generally

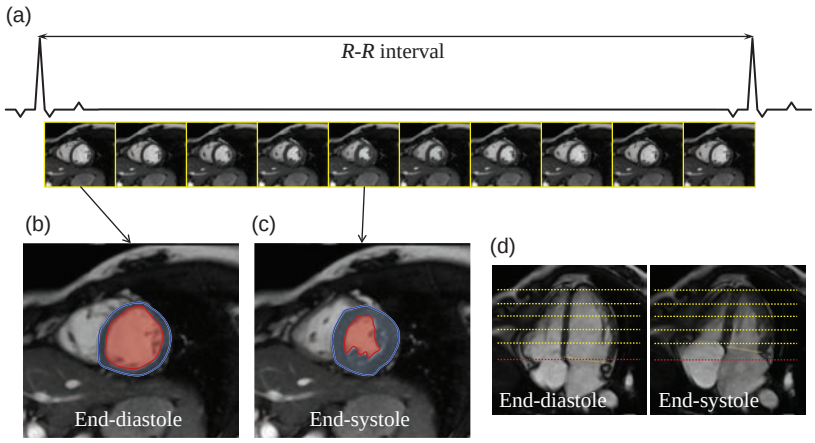

Figure 16.9 Functional cardiac analysis. (a) Ten phases from a single-slice cine acquisition in the short axis. (b) The largest ventricular volume is at end-diastole and (c) the smallest ventricular volume is at end-systole. The endocardial (red) and epicardial (blue) borders have been outlined on both phases. The left ventricular blood-pool is shaded red, while the ventricular muscle volume is shaded blue. Measurement of ventricular volume and mass requires outlining the borders on all the end-diastolic and end-systolic slices (dotted lines) in (d). Care should be taken when evaluating the most basal slice (dotted red line) since the longitudinal shortening of the heart during systole means that the most basal slice may not be in the ventricle.

necessary to sacrifice some spatial resolution. The development of both spatial and temporal parallel imaging techniques as discussed in Chapter 14 has also helped with the development of real-time cine imaging.

16.4.5 Functional Cardiac Analysis

If our short-axis stack of cine slices covers the entire left ventricle then we can measure the volume of the blood-pool at the end-systolic (smallest ventricular volume) and end-diastolic (largest ventricular volume) phases and calculate the percentage of blood ejected in each heartbeat. This is known as the ejection fraction (EF), and is an important measure of cardiac function. Specialized cardiac processing software can be used to either manually or (semi-)automatically define the endocardial border between the blood-pool and the myocardium, as shown in Figure 16.9. Summing the left ventricular blood-pool volume (blood-pool area × slice thickness) across all slices acquired at the end-diastolic phase gives the end-diastolic volume (EDV). Similarly, summing all the volumes at the end-systolic phase gives the end-systolic volume (ESV). The stroke volume, the volume of blood ejected during each heartbeat, is then calculated as the difference between EDV and ESV.

$$\mathrm{SV} = \mathrm{EDV} - \mathrm{ESV}$$

The ejection fraction (EF) as a percentage can then be calculated from

$$\mathrm{EF} = \frac{\mathrm{SV}}{\mathrm{EDV}} \cdot 100\%$$

If we also define the outer contour of the myocardium, called the epicardial border, we can then measure the volume of the myocardium. Multiplying the myocardial volume by the density of tissue (1.06 g ml^{-1}) gives us an estimate of the myocardial mass. This is another quantitative metric that can be used to monitor patients who have thickened ventricular walls.

With both endocardial and epicardial borders defined in the software, we can go still further and estimate regional function of the heart. In order to calculate these measures, the software (semi-) automatically calculates the centre-line midway between the endo- and epicardial borders. Short lines known as 'chords' which are perpendicular to the mid-line are then defined. The length of these chords can be displayed graphically, showing either their length at a particular phase, i.e. 'systolic wall thickness' or the difference in thickness between systole and diastole, i.e. 'wall thickening'. When this type of analysis is performed on all of the multi-slice short axis data it is usually displayed as a 'bull's-eye plot', a set of concentric rings with the inner-most ring representing the apical slice and the outermost ring the most basal slice. The metric is then usually represented as a colour scale. Figure 16.10 shows a regional left ventricular analysis in a patient with a thickened, i.e. hypertrophic, left ventricle.

16.4.6 Quantitative Velocity and Flow Imaging

Functional cardiac imaging includes quantitative imaging of blood flow, a powerful technique for assessing cardiac pathologies such as valvular regurgitation, ventricular shunting and quantifying

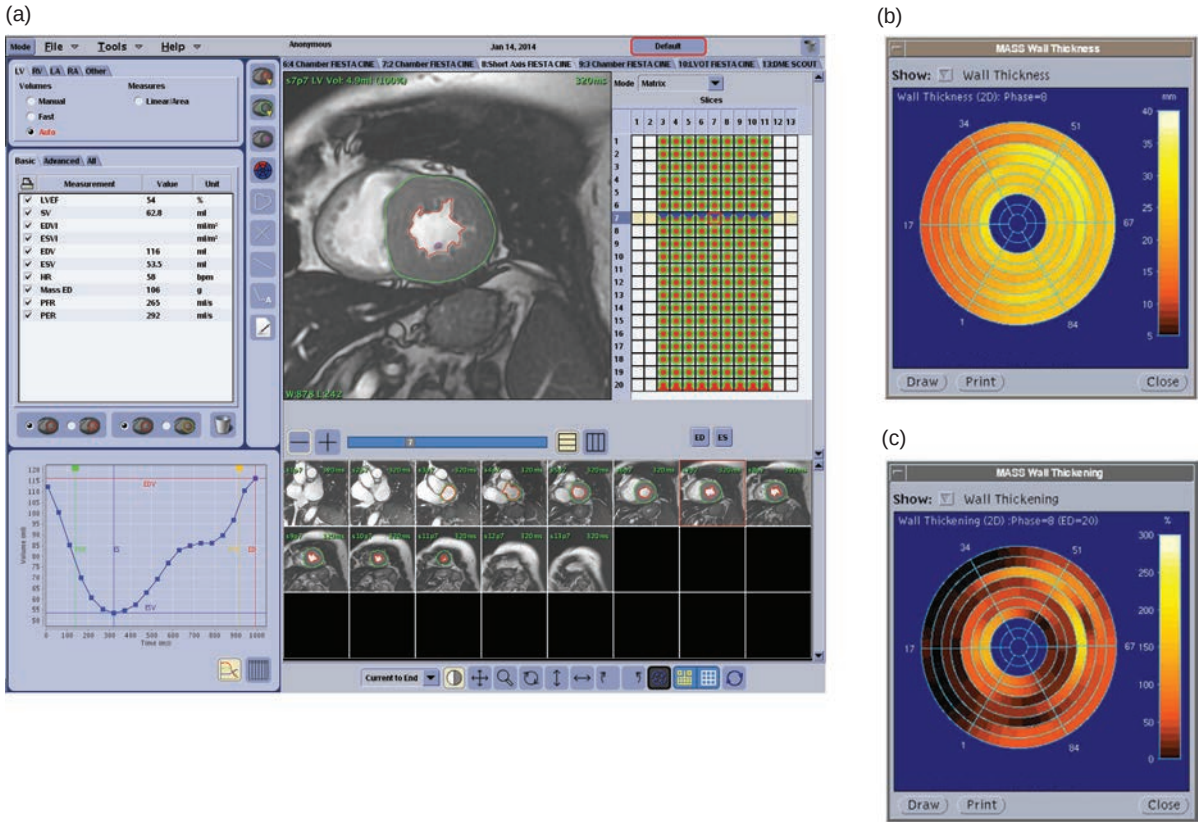

Figure 16.10 Regional left ventricular functional analysis. (a) The endo- and epicardial borders have been outlined on all the slices and phases from the short axis cine acquisition. The curve at the bottom left shows the ventricular volume time curve and the table above reports a stroke volume (SV) of 62.8 ml, ejection fraction (EF) of 54% and end-diastolic (ED) myocardial mass of 106 g. In a different patient with myocardial hypertrophy (b) shows a bull's-eye plot of the end-systolic wall thickness, demonstrating gross thickness of the entire left ventricle. (c) A bull's-eye plot can also show the change in wall thickness between end-systole and end-diastole. The plot shows general ventricular dysfunction with the septal region, in particular, showing poor contractility.

stenotic valves. In the last chapter we explained how it is possible to encode the velocity of moving spins using phase contrast imaging techniques. In quantitative velocity/flow imaging we usually perform a single-slice cine phase contrast (CPC) acquisition perpendicular to the direction of the vessel or valve in which we wish to quantify the velocity. The velocity-encoding gradients are usually applied along the slice-selection direction in order to quantify velocities through the slice, and the two encodings are usually interleaved within the same heartbeat to minimize spatial misregistration as shown in Figure 16.11. Like cine bSSFP functional imaging, CPC acquisitions can also be combined with segmented k-space acquisitions, retrospective gating and variable view-sharing techniques to reduce the overall acquisition time.

Figure 16.12 shows images from a typical CPC acquisition through the ascending aorta. If the instantaneous flow is plotted against time for all the temporal phases, then the area under the curve represents the blood flow in one heartbeat and is known as the stroke volume. Multiplying the stroke volume by the heart rate gives the volume of blood ejected in one minute, which is known as the cardiac output (ml min^{-1}). Figure 16.13 shows a CPC study in a patient with severe aortic regurgitation. The CPC slice was positioned perpendicular to the ascending aorta, just above the aortic valve. The area under the positive flow part of the curve (shaded green) represents the volume of blood ejected by the left ventricle in one heartbeat, while the area under the negative part of the curve (shaded red) represents the volume of blood that regurgitates back into the ventricle.

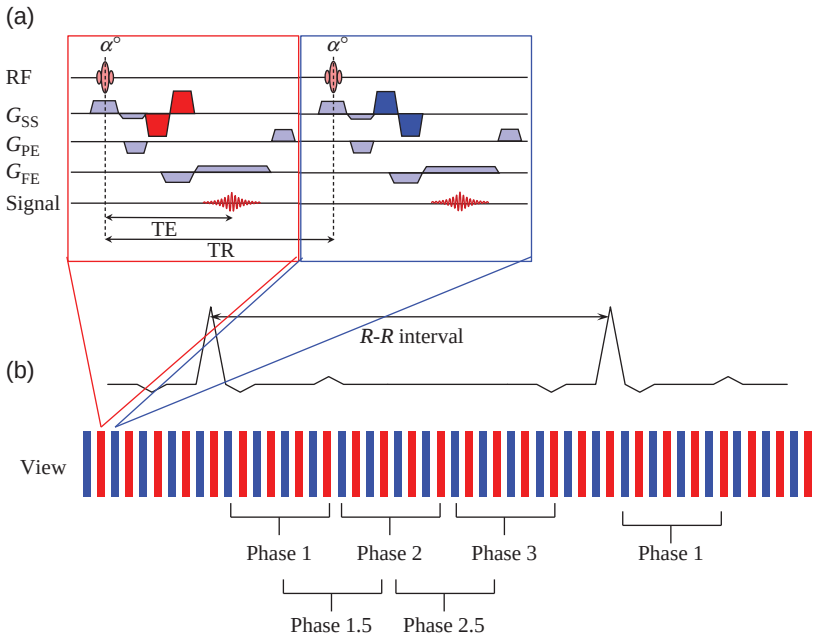

Figure 16.11 Cine phase contrast. The gradient-echo sequence (a) incorporates additional bipolar gradients to encode velocity into signal phase. The two encodings (red and blue) are usually performed in subsequent TRs. In this example the encodings are applied along the slice-select direction to encode velocity through the slice. In (b) the encodings are shown as part of a retrospectively gated segmented k-space acquisition. Multiple phase encoding steps or views are acquired in each *R–R* interval. In this case four views are acquired for each of the two encodings. Since the temporal resolution is 8 × TR in this example, we can use symmetric view sharing to improve the apparent temporal resolution as shown.

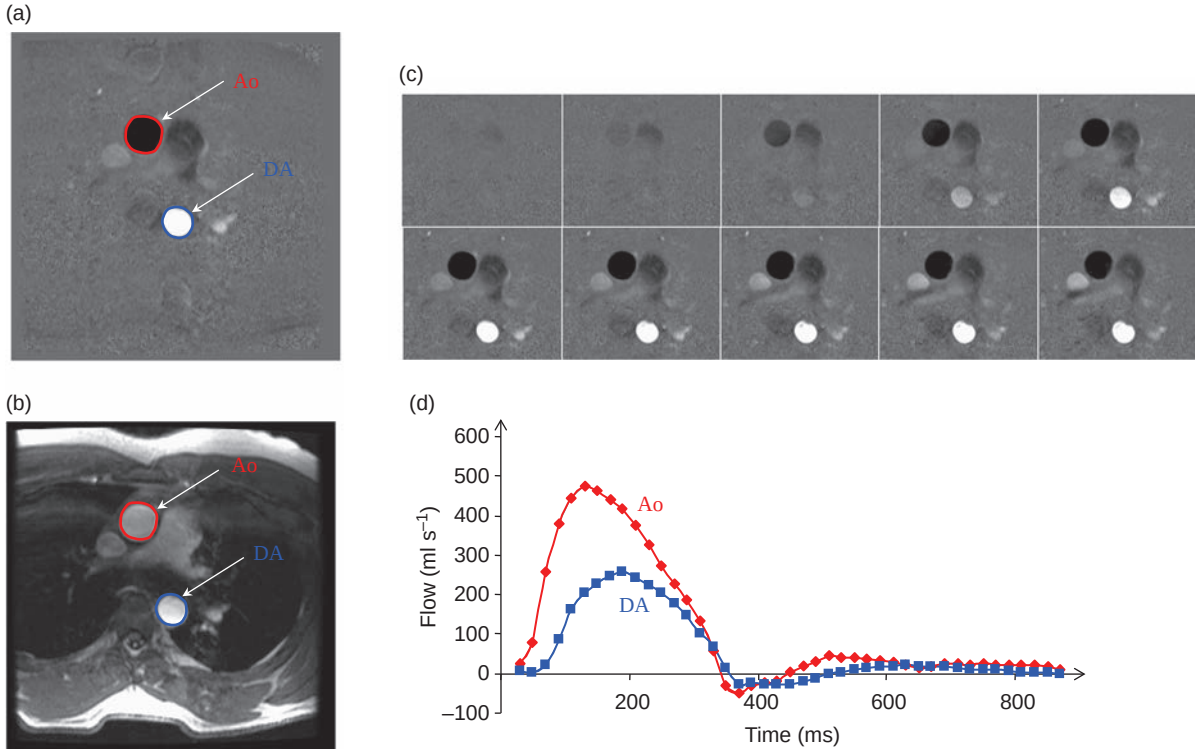

Figure 16.12 Cine phase contrast imaging through the ascending aorta (Ao). (a) The phase/velocity image and (b) the magnitude image from a single temporal phase. The velocity in the Ao is shown as shades of mid-grey to black, while velocity in the opposite direction in the descending aorta (DA) is shown as shades of mid-grey to white. Regions of interest (ROI) for both vessels have been outlined. (c) The first ten temporal phases of the phase/velocity images, giving (d) the flow vs time curve. The flow at each temporal phase is obtained by multiplying the average velocity in each ROI (mm s^{-1}) by the area of the ROI (mm^2) to give a flow in mm^3 s^{-1} or ml s^{-1}.

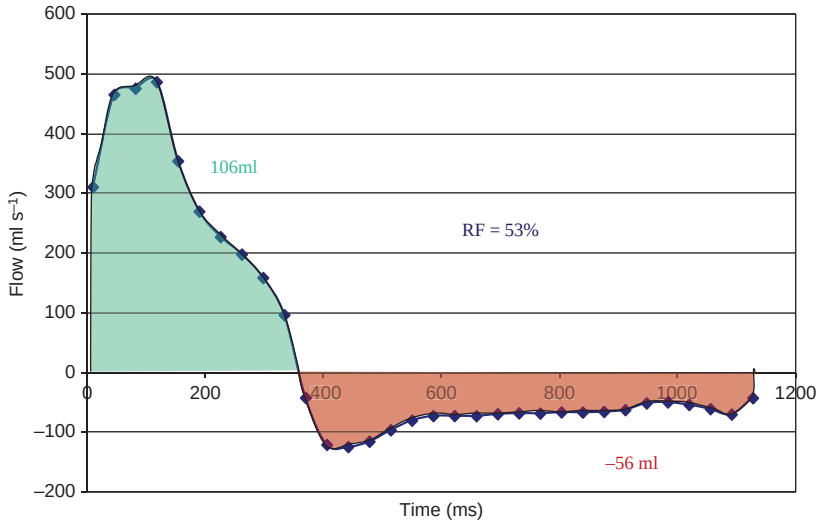

Figure 16.13 A flow–time curve obtained in the aorta of a patient with aortic regurgitation. There is a large forward flow during systole (green area under the curve) of 106 ml. During diastole approximately 56 ml of blood (red area under the curve) then flows back into the ventricle. This patient therefore has a regurgitant fraction (RF) of approximately 53%.

Remember from Chapter 15 that the user-defined velocity encoding (*venc*) parameter sets the velocity for which a 180° phase shift occurs. If the actual velocity exceeds the *venc* then aliasing will occur. This can be observed as a sharp transition from either black to white or white to black, as shown in Figure 16.14. If your analysis software supports the capability then it is possible to 'unwrap' this aliasing, otherwise it will be necessary to repeat the acquisition using a higher *venc*. You might think it's more sensible to select a very high *venc* to avoid the possibility of aliasing, but velocity images have velocity-to-noise ratio (VNR), just like standard images have an SNR. Therefore, velocity images will appear noisier as the *venc* is increased.

Even though the phase images from positive and negative flow encoding are subtracted to eliminate background phase errors, there may be residual errors due to the different eddy currents produced by the different flow-encoding gradient polarities. These errors appear as offsets in the data, so typically the stationary background is no longer zero. Correction of the data using the background signal offset may therefore be required.

Velocity mapping can also be performed in-plane by applying the flow-encoding gradients on the appropriate axis. Furthermore, like 3D phase contrast angiography, it is possible to acquire velocity data along all three directions, which when combined as part of an ECG-triggered 3D acquisition can provide 4D velocity quantification. These data can then be used to calculate temporally resolved 3D flow streamlines such as the example shown in Figure 16.15. These acquisitions are quite time consuming and require respiratory gating, typically using navigators.

Imaging Myocardial Strain

Qualitative review and quantitative analysis of cine cardiac images is widely used to demonstrate impaired myocardial wall contractility which is an important diagnostic and prognostic indicator of coronary heart disease. While it is easy to see the relative motion of the endo- and epicardial borders it is not possible, with standard cine imaging, to observe transmural myocardial motion, i.e. motion within the myocardium itself. However, there are a number of unique MRI techniques that can actually image myocardial strain, i.e. quantitatively measure the deformation within the myocardium. The most common method used for this application is 'tissue tagging'. A binomial combination of RF pulses and gradients, e.g. 1:–2:1 are applied immediately after every R-wave, and are then followed by a cine imaging sequence. The combination of RF pulses and gradients, known as SPAMM (**SPA**tial **M**odulation of **M**agnetization), temporarily superimposes a regular signal modulation pattern on to the images. These tags are typically applied in the form of either a 1D

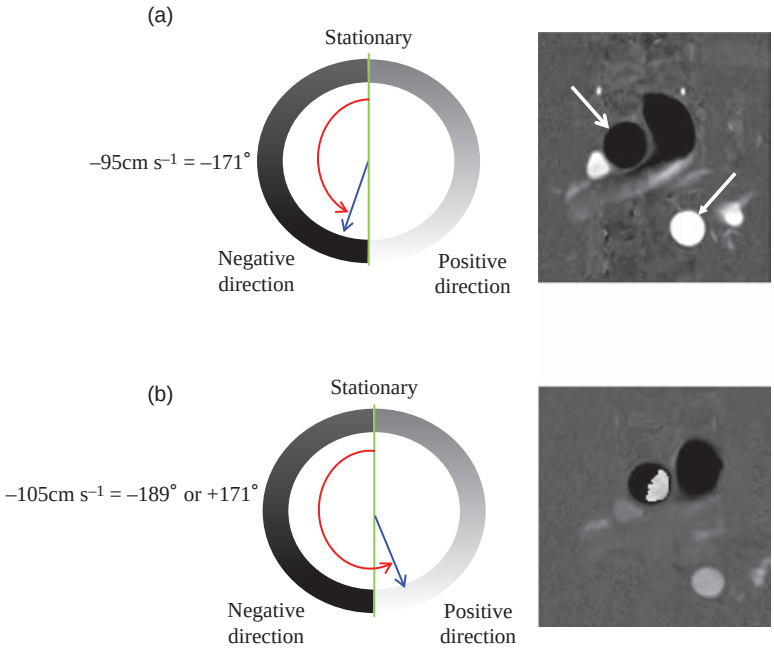

Figure 16.14 Phase contrast velocity aliasing. Velocities in one direction are allocated the range 0° to 180° and velocities in the opposite direction 0° to –180°. As a greyscale 0° is represented by mid-grey, while +180° is allocated white and –180° is allocated black. In (a) velocities in the ascending aorta (upper left arrow) are shown as shades of mid-grey to black, while velocities in the descending aorta (velocity is in the opposite direction) are shown as shades of mid-grey to white (lower right arrow). In (a) the *venc* is set to 100 cm s^{-1} so a velocity of –95 cm s^{-1} results in a phase shift of –171°. However, if the velocity exceeds the *venc* then the data will appear aliased (b). In this case with a *venc* of 100 cm s^{-1} a velocity of –105 cm s^{-1} results in a phase shift of –189°. Since this is greater than 180° the reconstruction makes it appear as +171°. In this case the velocity in part of the ascending aorta exceeds 100 cm s^{-1} and part of the aortic signal appears aliased with a sudden transition from black to white.

(lines) or a 2D (grid) structure as shown in Figure 16.16. As the myocardium moves and deforms throughout the cardiac cycle, the tagging pattern also deforms to visually demonstrate regions of normal and impaired contractility. Various image processing techniques can then be used to track the tag displacements and calculate the strain as well as ventricular torsion – the twisting of the ventricle as it contracts. HARP (**HAR**monic **P**hase) is a particular method that can rapidly analyse tagged images and create parametric images demonstrating the motion of every material point within the myocardium. More recently methods such as DENSE (**D**isplacement **EN**coding with **S**timulated **E**choes) have been used to encode tissue displacement into signal phase from which the strain can then be calculated, while the SENC (**S**train **ENC**oding) technique directly produces images of tissue strain. In addition, conventional cine phase contrast techniques can also be used to encode in-plane and through-plane myocardial wall velocity. The velocity information can then be integrated over time to determine tissue displacement and subsequently calculate the strain.

16.5 Myocardial Perfusion

MRI offers a number of advantages over the conventional nuclear medicine methods for the evaluation of myocardial perfusion, including improved spatial resolution, the absence of overlying tissue attenuation effects as well as an absence of ionizing radiation. Clinical myocardial perfusion MRI involves imaging the heart during the bolus administration of Gd-based contrast agent, during which we observe a transient T_1-enhancement effect whereby the myocardial signal intensity increases during the passage of the contrast agent through the myocardium. Regions of ischaemia with poor perfusion will show a significantly reduced and/or delayed enhancement compared to the normally perfused regions. Note that at the time of writing, Gd-enhanced MRI of the heart is an off-label use for all FDA-approved gadolinium-based contrast agents.

Since the first pass of the contrast agent through the myocardium is very rapid, typically 10 s or less, the imaging requirements are extremely demanding. Ideally we would like to get whole-heart coverage with a temporal resolution of one heartbeat, however we can really only achieve 3–4 slices per heartbeat. The basic sequence is therefore a very short TR gradient-echo sequence with an acquisition time of less than 200 ms. A non-selective 90° saturation pulse is applied prior to the imaging sequence, which increases the sensitivity for changing T_1s. The saturation pulse also provides a degree of arrhythmia insensitivity to allow for any differential signal recovery if the heart rate varies. Figure 16.17 shows one phase from a multi-slice imaging acquisition using an interleaved gradient-echo planar imaging sequence. This study shows a region of sub-endocardial ischaemia as an area of reduced

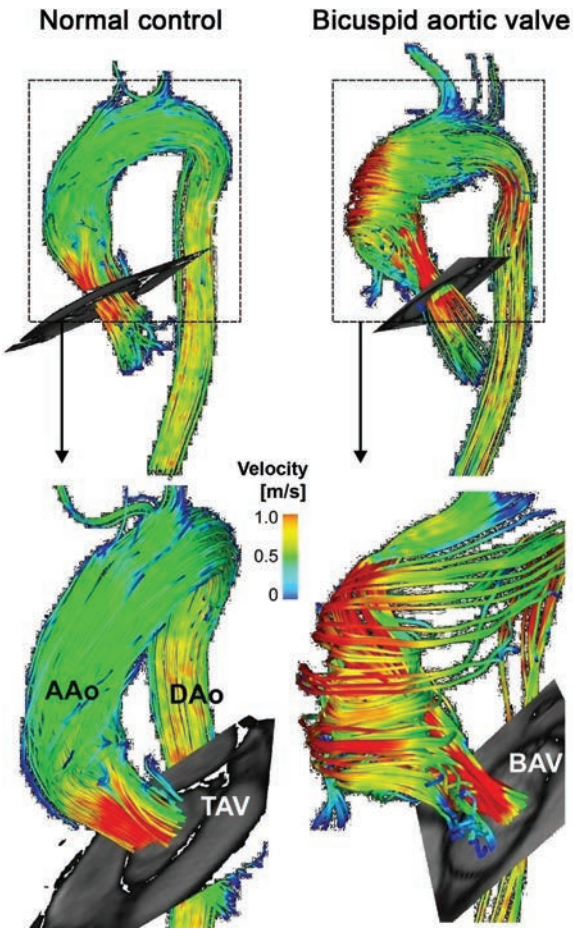

Figure 16.15 3D velocity streamlines calculated from 4D phase contrast data encoded in all three orthogonal directions. The individual lines represent traces along the instantaneous velocity vector field in a systolic phase. The colour scale represents the velocity in m s^{-1}. The figure shows the difference in flow patterns from two subjects; one with a normal tricuspid aortic valve (TAV) and one with a congenitally abnormal bicuspid aortic valve (BAV). Courtesy of Dr Michael Markl, Northwestern University, Chicago.

contrast agent uptake. Care must be taken in viewing these perfusion images to ensure that apparent perfusion 'defects', particularly those in the sub-endocardium, are not actually due to susceptibility effects from the high concentration of contrast agent in the left ventricle during the first pass, or motion artefacts due to the myocardium moving during the readout period.

Stress Testing

Patients usually feel the typical symptoms of ischaemic heart disease, such as chest pain, when they physically exert themselves. This is because in the resting state the coronary arteries can deliver sufficient blood flow to the heart, but during exertion they may not be able to deliver the increased blood flow required by the myocardium, hence the pain. Similarly, if we perform a myocardial perfusion scan in the resting state there may not be any noticeable regional differences in blood flow. It is necessary therefore to 'stress' the patient by increasing the myocardial blood flow. While exercise is the best way to achieve this, it is not easy to do in an MRI scanner. Alternative methods include using drugs, like adenosine, that can transiently increase myocardial blood flow while the perfusion sequence is running. Some centres also like to perform a resting state perfusion scan as well. That way any apparent perfusion defects that appear on both stress and rest images can be identified as artefacts and real perfusion defects will only be seen on the stress images.

Quantitative Perfusion Imaging

Perfusion images are usually reviewed qualitatively, with true perfusion defects usually persisting for at least a few heartbeats while also following the boundaries of the feeding coronary artery territories. While qualitative analysis has demonstrated good sensitivity and specificity compared to conventional radionuclide techniques, there have been some studies of semi-quantitative indices that may offer improved sensitivity and specificity. A popular method is to compare the maximum upslope of the myocardial signal intensity curves at both stress and rest in order to calculate a myocardial perfusion reserve index (MPRI). However, since the patient's general cardiac function may be very different between rest and stress, the data are usually normalized to the upslope of the signal in the left ventricular blood-pool. More sophisticated quantitative analysis methods have also been proposed, similar to those used for DCE-MRI.

A problem with all quantitative image analysis is the necessity to ensure that all the temporal phases are aligned. If the patient can hold their breath for at least the first 20–30 seconds then upslope analysis is fairly straightforward, otherwise each phase needs to be spatially co-registered. Analysis may be further confounded by ectopic beats that may occur in patients when undergoing pharmacological stress. Absolute quantification of myocardial perfusion in ml g^{-1} min^{-1} of tissue is complicated by the fact that using standard contrast doses, e.g. 1.0 mmol kg^{-1}, the signal intensity is not linearly related to the

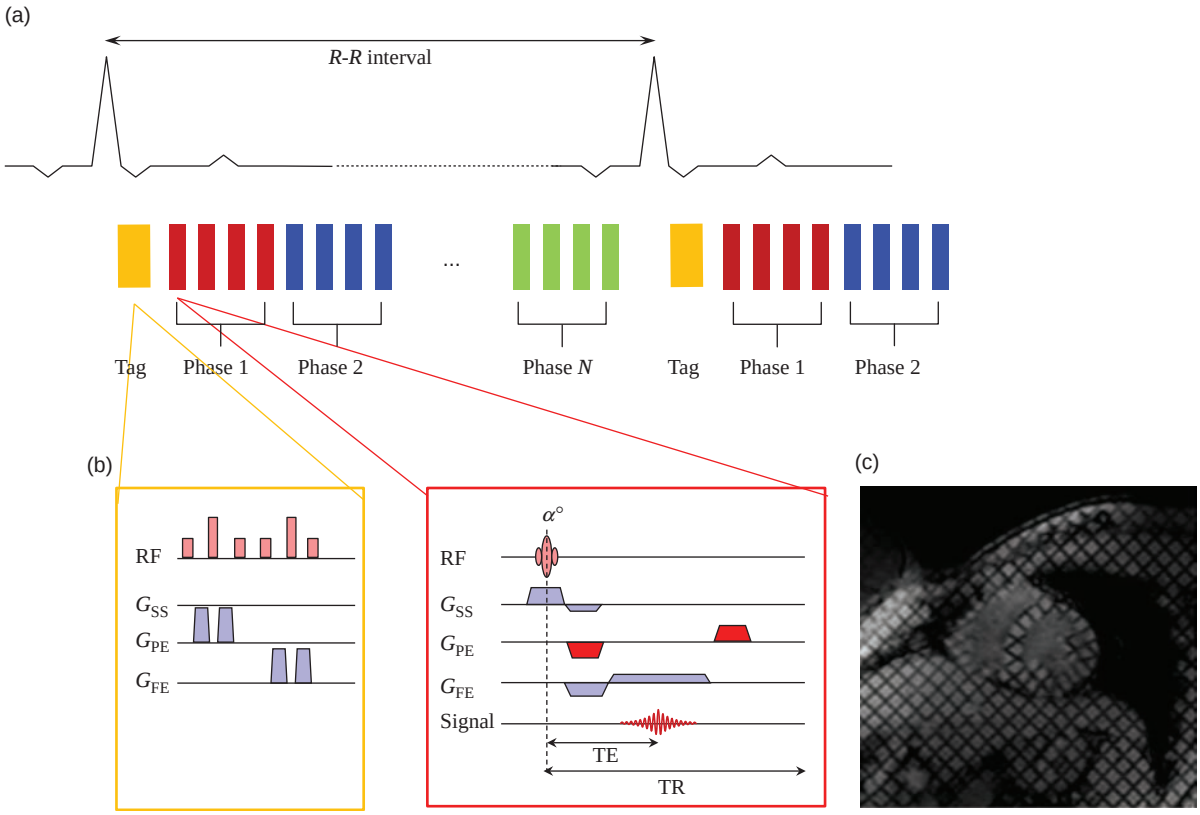

Figure 16.16 Myocardial tagging. (a) Prospectively triggered segmented k-space acquisition which is preceded by a myocardial tagging module (b). The 1:–2:1 tagging module creates a spatial modulation of the signal, i.e. a regular grid pattern, at the start of the cardiac cycle. As the heart twists and deforms throughout the cardiac cycle, the tag lines will distort accordingly. (c) One frame from a tagging cine loop demonstrating transmural myocardial motion. Note that the tag lines fade through the cardiac cycle due to T_1 recovery.

contrast agent concentration. This has led some groups to use lower concentrations, e.g. in the range of 0.05–0.075 mmol kg^{-1}, where a linear relationship can be assumed. In addition, all clinically approved contrast agents distribute in both the vascular and extracellular space, affecting the amount of signal enhancement. Lack of knowledge about the relative volumes of these tissue spaces also contributes to the difficulties in absolute quantification.

16.6 Myocardial Viability

A myocardial infarction, or 'heart-attack', occurs when there is insufficient blood flow to a part of the myocardium resulting in tissue damage due to insufficient oxygen. The damage may be either permanent, i.e. a myocardial infarction, or reversible, in which case the tissue is still viable and function may be restored with suitable revascularization. It is therefore very important to be able to determine whether a region of dysfunctional myocardium is either viable or infarcted.

One way to identify viable myocardium is to perform cine imaging while increasing the dose of a pharmacological agent such as dobutamine which increases myocardial contractility. Any myocardial tissue with a wall motion abnormality at rest and which subsequently improves with low-dose dobutamine is regarded as viable. Further increases in the dobutamine dose results in the myocardium becoming ischaemic and ceasing to contract.

An alternative and extremely powerful approach is the direct imaging of non-viable myocardial regions using Late Gadolinium Enhancement (LGE). Recent evidence shows that LGE is exclusively related to irreversible injury, irrespective of contractile function or age of injury. After either an acute ischaemic injury or a chronic infarction there is an increase in the

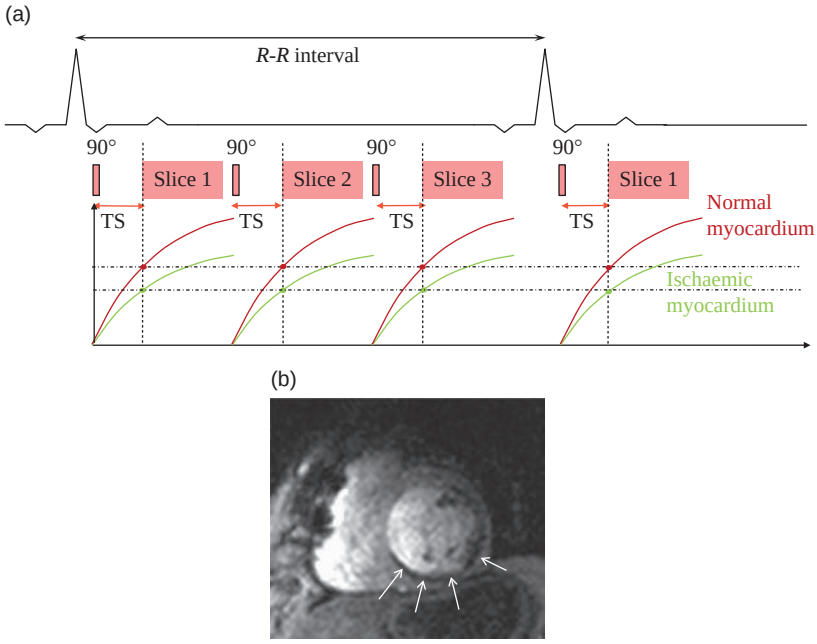

Figure 16.17 Myocardial perfusion imaging. (**a**) Each slice acquisition comprises a very fast ECG-triggered T_1w sequence. A small number of slices are repeatedly acquired during each *R–R* interval. Prior to each acquisition a non-selective 90° saturation pulse is applied. During the saturation recovery time (TS) the magnetization recovers due to T_1 recovery. The contrast agent, which was injected at the start of the acquisition, will flow into the normally perfused myocardium, causing the signal to recover more rapidly (red curves showing enhanced myocardium). Ischaemic myocardium will show a diminished uptake of the contrast agent. (**b**) One slice from a myocardial perfusion study showing a sub-endocardial perfusion defect (arrows) compared to normally enhancing myocardium. The 90° pulse ensures that all the longitudinal magnetization recovery starts from zero. This makes the sequence robust to cardiac arrhythmias where the *R–R* intervals may vary in length, resulting in variable signal intensity.

extracellular volume which results in retention of a standard extracellular gadolinium contrast agent. In acute infarcts the loss of cell membrane activity allows the contrast agent to accumulate in the extracellular space, while in chronic infarcts the cardiomyocytes are replaced by fibrotic tissue that has a smaller intracellular space compared to the extracellular space. If T_1w imaging is performed 10–20 min following administration of the contrast agent there is maximal signal difference between infarcted and normal myocardium.

To maximize visualization of the infarct the imaging sequence of choice is an inversion-recovery prepared gradient-echo acquisition in which the inversion time (TI) is optimized to null the signal from normal myocardium as shown in Figure 16.18. The choice of TI can be somewhat tricky and various approaches have been developed over the years. First, rapid, low spatial resolution, LGE images can be obtained at different TIs to visually assess which yields the minimal signal in normal myocardium. Second, TI 'scout' sequences have been developed which employ a single inversion pulse followed by multiple low spatial resolution gradient-echo readouts, each effectively acquired at an increasing TI. Finally, sequences that retain the sign of the inverted magnetization, so-called **P**hase **S**ensitive **I**nversion **R**ecovery (PSIR), have been developed. PSIR images maintain good normal/infarcted tissue contrast over a wider range of TIs than the magnitude-reconstructed standard IR sequences.

Infarct Imaging

If a cine study shows a region of wall motion abnormality that is 'bright' and transmural on LGE imaging, then the myocardium will not recover function following revascularization. Conversely, if the wall motion abnormality does not demonstrate hyperenhancement on LGE then this most probably represents viable tissue that is likely to recover function after revascularization. The technique is sometimes

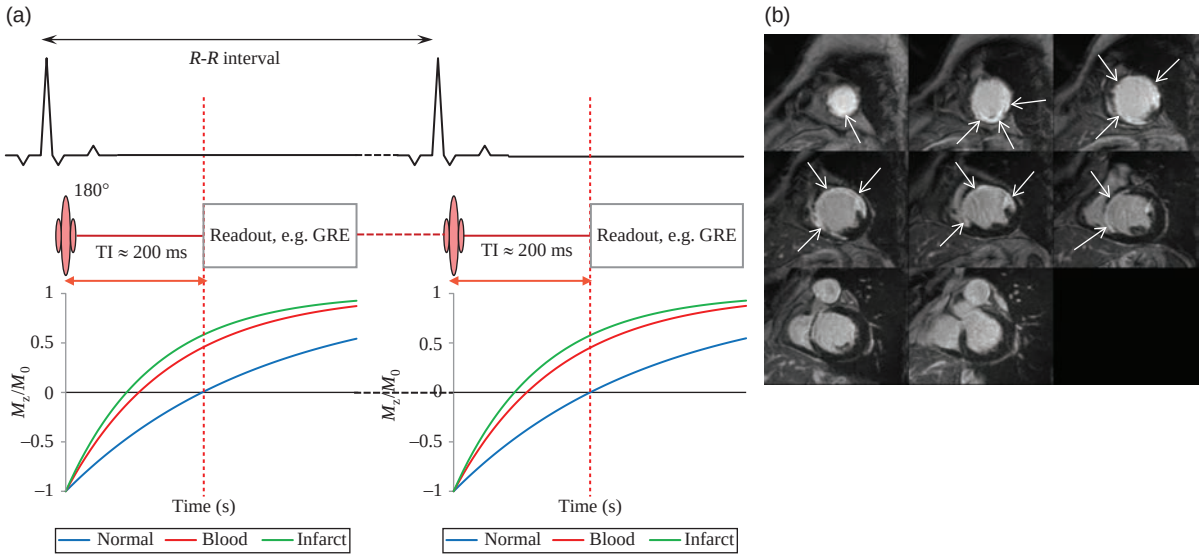

Figure 16.18 Late gadolinium enhancement imaging. (a) A 180° pulse inverts the magnetization which then recovers. If the correct TI is chosen, then when the centrically ordered segmented GRE sequence is played out the signal from the normal myocardium should be zero while the signal within the infarcted tissue is hyperintense, as shown by the arrows in (b).

called 'infarct sizing', since the region of hyper-enhancement correlates with the region of infarction. The transmural extent of myocardial enhancement has been shown to predict the probability of functional recovery. Figure 16.18 shows a set of myocardial delayed enhancement images with a very large region of hyper-enhancement.

While LGE works well for identifying chronic infarcts, early gadolinium enhancement (EGE), with imaging around two minutes after contrast injection, can be used to detect acute myocardial infarction. In this situation the hyper-enhancement represents regions of dead myocardial cells due to compromised myocardial blood flow at the capillary level, despite having a patent coronary artery. This is termed microvascular obstruction (MVO) or 'no-reflow' and is an important prognostic indicator for future cardiac events.

It should be noted that fibrosis, and hence LGE, can also occur in a number of other non-ischaemic cardiac muscle diseases (cardiomyopathies).

16.7 Myocardial Tissue Characterization

Relaxation times of the myocardium are altered in various disease states due to changes in water content as well as the local molecular environment. Elevated T_1 has been reported in a number of cardiac diseases and the measurement of T_1 pre- and post-contrast can be used to measure diffuse myocardial fibrosis. Quantitative T_2 imaging has the potential to improve the accuracy and reliability of oedema imaging compared to T_2-STIR imaging. Myocardial iron overload is a common finding in iron storage diseases like β-thalassaemia. The response to chelation therapy may be monitored using quantitative MRI techniques, most notably T_2^* mapping, since this method can assess tissue iron concentrations over a wide range. These methods, and their advantages and disadvantages, are explained fully in Chapter 19.

16.8 Coronary Artery Imaging

The visualization of the coronary arteries using MRI presents numerous technical challenges. Coronary vessels have small lumens, follow tortuous paths within the epicardial fat and move significant distances during the cardiac and respiratory cycles. The simplest approach to coronary MRA is to use breath-hold (segmented k-space) gradient-echo imaging with a short acquisition window in diastole. Multiple 2D slices with fat saturation are prescribed parallel to the coronary vessel. While this method can produce good results, complete coverage generally requires multiple breath-holds, and the slice thickness limits the spatial resolution achievable.

Better results can be obtained using ECG-gated 3D-bSSFP sequences that produce a high signal from blood. T_2 preparation schemes and fat suppression are often used to reduce myocardial muscle and fat signal respectively. The extended imaging time generally makes breath-holding impractical and thus respiratory gating is required. This is usually performed using navigators. The navigator signal may be used to gate the data either prospectively, i.e. before data acquisition, or retrospectively, i.e. after data acquisition but before image reconstruction.

While MR coronary angiography can be used for looking at the proximal coronary arteries, CT angiography is far quicker and more robust for assessing the whole of the coronaries.

Further Reading

Biglands JD, Radjenovic A and Ridgway JP (2012) 'Cardiovascular magnetic resonance physics for clinicians: part II'. *J Cardiov Magn Reson* 14:66. Available online at www.jcmr-online.com/content/14/1/66 [accessed 7 May 2015].

Coelho-Filho OR, Rickers C, Kwong RY and Jerosch-Herold M (2013) 'MR myocardial perfusion imaging'. *Radiology* 266:701–715.

Doltra A, Amundsen BH, Gebker R, Fleck E and Kelle S (2013) 'Emerging concepts for myocardial late gadolinium enhancement MRI'. *Current Cardiology Reviews* 9: 185–190.

Kwong RY (ed.) (2008) *Cardiovascular Magnetic Resonance Imaging*. Totowa, NJ: Humana Press.

Ridgway JP (2010) 'Cardiovascular magnetic resonance physics for clinicians: part I'. *J Cardiov Magn Reson* 12:71. Available online at www.jcmr-online.com/content/12/1/71 [accessed 7 May 2015].